

## Measurement of Film Thickness by Double-slit Experiment

Soobong Park, Byoung Joo Kim, Deok Woo Kim, and Myoungsik Cha\*

*Department of Physics, Pusan National University, Busan 46241, Korea*

(Received September 29, 2020 : revised November 30, 2020 : accepted December 30, 2020)

We show that a simple double-slit experimental setup can be used to measure the thickness of a transparent thin film. The phase difference between the light passing through one slit covered with photoresist film and that passing through the other slit without film was estimated using the simple Fraunhofer diffraction formula for a double slit. Our method gave error of a few percent or less for film thicknesses ranging from 0.7 to 1.7  $\mu\text{m}$ , demonstrating that a laboratory double-slit experimental setup can be utilized in practical film-thickness measurements.

*Keywords* : Diffraction, Double-slit, Thickness, Thin film

*OCIS codes* : (120.2650) Fringe analysis; (120.5050) Phase measurement; (310.0310) Thin films

### I. INTRODUCTION

Light interference with double slits is a conclusive experiment in proving the wave nature of light. (Although Thomas Young did not actually use double slits in his paradigm-changing experiment, double-slit experiments are generally called “Young’s experiments”. Instead of double slits, he used a thin cardboard to split the wavefront of the incoming light beam [1].)

Double-slit experiment utilizes a wavefront-division scheme to produce interference. In terms of efficiency or brightness of fringes, often amplitude division using a beam splitter is advantageous, while in some cases, as in this study, wavefront division can be useful. Although this experiment is familiar to most researchers and students in various fields of science and engineering, its applications in measurements seem to be rare. We could find only a few examples: Kim *et al.* [2] developed a method for inspecting the thickness uniformity of glass plates, and Emile *et al.* [3] studied the Marangoni effect in soap films based on double-slit experiments.

Another example of the application of double-slit interference is wavelength measurement. Since the fringe spacing of a double-slit interference pattern is determined by the slit separation  $s$  and the wavelength  $\lambda$  of the incident

monochromatic light  $\lambda$ , such a simple experimental setup can be utilized as a wavelength meter. Amazingly, the resolving power was estimated to be  $2s/\lambda$ , which can be as large as 4,000 under ideal circumstances [4]. Although this is overestimated because in practice one cannot measure the fringes in the entire half-space ( $-90^\circ$  to  $+90^\circ$ ), a simple double-slit apparatus seems to be a perfect tool for demonstrating the principles of interferometric measurement of wavelength and other parameters, such as film thickness.

There are diverse methods for measuring the thickness of a thin film, including mechanical scanning of a probe, Michelson interferometry, electron microscopy, and waveguide (WG) coupling through a high-index prism. Each method provides fairly accurate results, together with some limits. In the mechanical-probe scanning method, probe-surface contact is essential; therefore, a large error may be involved in the thickness measurement of soft films or very thin films due to scratching of the surface, even with a very light probe. An electron microscope can accurately measure very small thicknesses, but a disadvantage is that it takes a lot of effort to prepare a sample with a nice cross section. The Michelson interferometer has advantages such as no mechanical contact and easy sample preparation [5]; a disadvantage is that it is sensitive to mechanical vibrations. The WG-coupling method has the great advantage of

\*Corresponding author: [mcha@pusan.ac.kr](mailto:mcha@pusan.ac.kr), ORCID 0000-0002-5997-3881

Color versions of one or more of the figures in this paper are available online.



This is an Open Access article distributed under the terms of the Creative Commons Attribution Non-Commercial License (<http://creativecommons.org/licenses/by-nc/4.0/>) which permits unrestricted non-commercial use, distribution, and reproduction in any medium, provided the original work is properly cited.

providing accurate values of thickness and refractive index simultaneously [6]; however, a disadvantage is that very thin films cannot be measured, because WG modes do not exist when the film is too thin.

In this report we propose a method to measure the phase change of the light waves passing through a thin film, which leads to an estimation of the thickness by using a very simple double-slit setup. A coherent light beam is illuminated on two slits almost in contact with a thin film coated on a transparent substrate. When the film is partially removed on the substrate area adjacent to one of the two slits, the interference/diffraction pattern changes from that obtained through a uniform reference plate, due to the phase difference between the two light waves passing through the two slits. A phase difference is obtained by comparing the diffraction pattern to that for the reference plate, from which one can evaluate the thickness of the thin film. We prove the validity of this method by comparing the results to the thickness values measured by a WG-coupling method.

## II. EXPERIMENTAL SETUP AND METHOD OF FRINGE ANALYSIS

In typical double-slit experiments, one needs twin slits separated by submillimeter distances to form an analyzable interference pattern on a screen placed a few meters away. In our experiment, however, it would not be easy to align the phase-step boundary line completely under the opaque region between the slits, for such a small slit separation. To circumvent this difficulty, we used slits spaced several millimeters apart.

A schematic diagram of our experimental setup is shown in Fig. 1. Instead of plane-wave illumination, a spreading laser beam from a point source (beam waist formed by the first lens L1) was incident upon the entire double-slit region (almost in contact with the sample), and the transmitted light was collected on a screen through the second lens L2. In the arrangement in which the image of the point source is formed on the screen, a Fraunhofer diffraction pattern of the double slits is obtained (see Appendix for details),

which makes simple, accurate analysis possible.

The phase delay of the light passing through the thin film can be evaluated by comparing the Fraunhofer diffraction pattern to that of a reference plate. At normal incidence the phase difference is given by

$$\phi = \frac{2\pi}{\lambda} (n_f - n_a) d, \quad (1)$$

where  $n_f$  and  $n_a$  are the refractive indices of the film material and the atmosphere respectively,  $d$  is the thickness of the film, and  $\lambda$  is the wavelength of the incident light in vacuum. Assuming equal and uniform illumination of each slit, the intensity distribution of the Fraunhofer diffraction as a function of diffraction angle  $\theta$  can be calculated as [2, 5]

$$I = I_0 \left( \frac{\sin \beta}{\beta} \right)^2 \cos^2 \left( \frac{\pi s}{\lambda} \sin \theta + \frac{\phi}{2} \right). \quad (2)$$

Here  $I_0$  is a constant,  $s$  is the slit separation (distance between the centers of the two slits),  $w$  is the width of each slit, and

$$\beta \equiv \frac{w\pi}{\lambda} \sin \theta. \quad (3)$$

For a uniform reference sample with  $\phi = 0$ , this equation renders the well-known symmetric double-slit Fraunhofer diffraction pattern shown in Fig. 2 [5].

Also in that figure, we plot the diffraction patterns of thin films with phase steps corresponding to two different values of  $\phi$  calculated by Eq. (1). For a nonzero phase step, the central maximum moves to one side, breaking the symmetry. When  $\phi = 2\pi$ , the diffraction pattern returns to that of the reference sample.

The maxima of diffraction occur when  $(\pi s/\lambda) \sin \theta + \phi/2 = m\pi$  ( $m = 0, \pm 1, \pm 2, \dots$ ). For the reference sample ( $\phi = 0$ ) the second maximum corresponds to  $(\pi s/\lambda) \sin \theta = \pi$ , from which one can determine the angle  $D$  between the principal maximum ( $\theta = 0$ ) and the second maximum. Since  $(\pi s/\lambda) \sin \theta = (\pi s/\lambda) \sin D = \pi$  [Eq. (3)], and assuming that the dif-

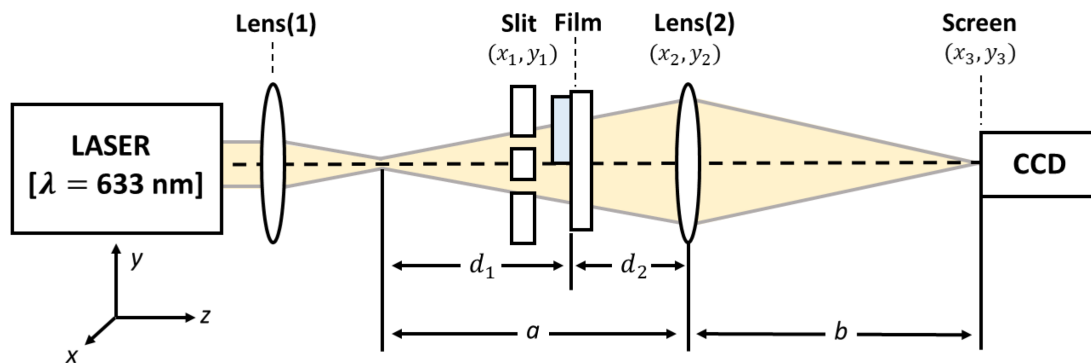
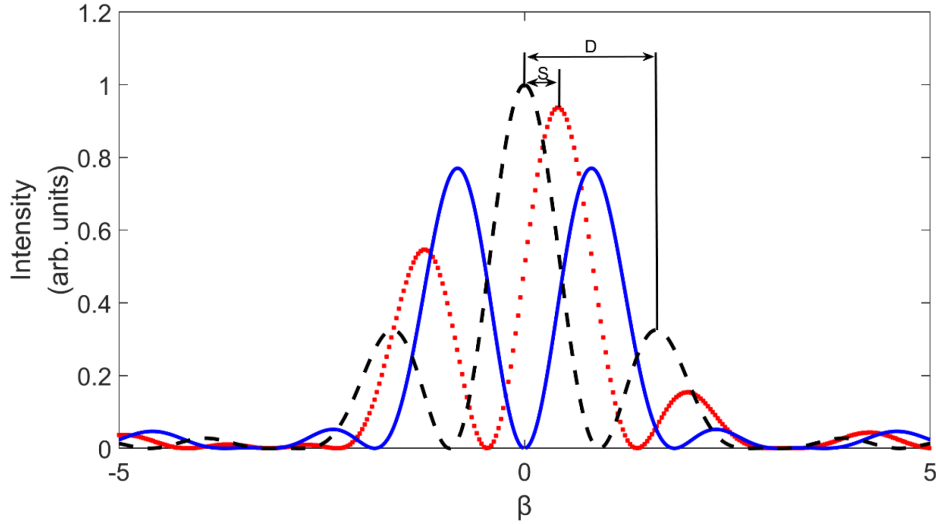


FIG. 1. Experimental setup.



**FIG. 2.** Calculated Fraunhofer diffraction patterns for phase steps of 0 (dashed line),  $\pi/2$  (dotted line), and  $\pi$  (solid line), with  $s = 3.9$  mm,  $w = 2.3$  mm, and  $\lambda = 633$  nm.

fraction angle is small, we obtain

$$D \approx \sin D = \frac{\lambda}{s}. \quad (4)$$

When there is a phase step, we set  $(\pi s/\lambda) \sin \theta + \phi/2 = 0$  in Eq. (2) to find the angular shift  $S$  of the principal maximum. Assuming again a small angular range of diffraction, we obtain

$$S = \theta \approx \sin \theta = \frac{-\phi\lambda}{2\pi s}. \quad (5)$$

It should be noted that the ratio between  $S$  and  $D$  results in the following simple relation:

$$\left| \frac{S}{D} \right| = \frac{\phi}{2\pi}. \quad (6)$$

Therefore, by measuring the relative angular shift  $S$  with respect to  $D$ , the phase difference  $\phi$  due to the presence of the film can be directly obtained. Finally, the thickness  $d$  is related to the phase difference by Eq. (1), when the refractive indices  $n_f$  and  $n_a$  are known. Such a relative measurement has a great advantage over absolute measurements of the diffraction parameters, which involve the accurate slit dimensions and the distance between the slits and the screen.

However, one obtains multiple possible values of the thickness, because phase differences of  $\phi$  ( $|\phi| < 2\pi$ ) and  $\phi + 2m\pi$  ( $m = 1, 2, 3, \dots$ ) would produce exactly the same diffraction patterns. This  $2\pi$ -phase-ambiguity problem can be circumvented by measuring the absorbance at one wavelength (usually in the ultraviolet) and comparing the thickness to that of a reference sample calibrated for a thickness-

absorbance relation (Here a rough estimate of the thickness range is enough).

In the discussion above, in locating the relevant maxima we neglected the factor  $(\sin \beta/\beta)^2$  in Eq. (2). Although we obtained a very simple and physically clear result (Eq. (6)) by neglecting the envelope, one can suspect that there could be slight modifications in the locations of the maxima in the real diffraction pattern. Therefore, we fit the experimental diffraction patterns to Eq. (2) in most of our subsequent analyses.

### III. EXPERIMENTS AND ANALYSES

Thin films of various thicknesses are made from a photoresist (Clariant, AZ5214E) by spin coating on fused-silica substrates (1 mm thick, 25.4 mm in diameter). For each coated sample, half of the film's area is exposed to a UV light, and then removed with a developer to form a phase step. For easy fabrication of double slits and alignment, two parallel slits of width  $w = 2.3$  mm are formed on a black acrylic plate with  $s = 3.9$  mm (the distance between the centers of the slits). The phase-step boundary line can be completely covered by the opaque region between the two slits, and a few interference fringes are contained within the major diffraction envelope with this configuration. A He-Ne laser beam is focused by the first lens L1, with a focal length of 125 mm, to form a beam waist, as shown in Fig. 1. The focal length of the second lens (L2) is 1 m, to form a diffraction pattern broad enough to cover the entire active region of a linear charge-coupled-device (ALPHALAS, CCD-S3600-D(-UV)) array placed at the screen plane.

Figure 3(a) shows the measured diffraction patterns of a phase step (sample #1) and a reference sample (uncoated fused-silica substrate). First we try to analyze the results roughly by reading  $D$  and  $S$  in units of pixels and estimat-

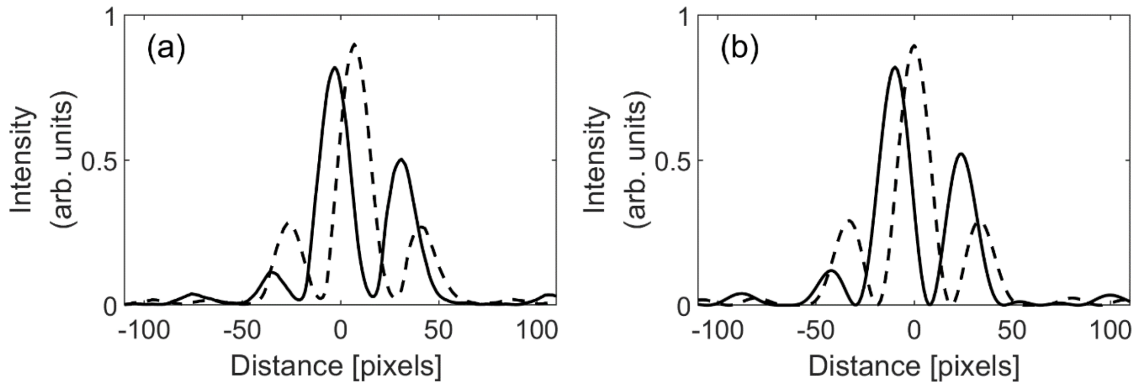


**FIG. 3.** Diffraction patterns. (a) Experimental diffraction patterns of sample #1 (solid line) and the reference sample (dashed line). (b) Calculated diffraction patterns corresponding to those in (a) with  $\phi = 1.42\pi$ .

ing the phase  $\phi$  using Eq. (6) (neglecting the envelope in Eq. (2)). We fit the maxima in the diffraction patterns to quadratic functions to determine their exact locations, from which we obtain  $D = 33.8$  and  $S = 24.0$ . By Eq. (6), the phase  $\phi$  is calculated to be  $1.42\pi$ , resulting in possible thicknesses of  $0.713, 1.72, 2.72 \mu\text{m}, \dots$  by Eq. (1), using the known values of the refractive indices of air ( $n_a = 1.00$ ) and our photoresist ( $n_f = 1.63 \pm 0.01$ , measured by the WG-coupling method described below). Since the photoresist we use has an absorption resonance at  $279 \text{ nm}$ , the approximate thickness range can be determined by comparing the absorbance of the thin film to that of a thin film of known thickness, resolving the  $2\pi$ -phase-ambiguity problem. In Fig. 4 a trend line is drawn by measuring the absorbance values at  $279 \text{ nm}$  for photoresist thin films with thicknesses of  $0.82, 1.04, \text{ and } 1.24 \mu\text{m}$ , measured by the WG-coupling method [6]. Since the absorbance value of sample #1 marked on this line indicates that the thickness lies in the range of  $0.7\text{--}0.8 \mu\text{m}$ , we conclude that the correct thickness is  $0.713 \mu\text{m}$ .

As plotted in Fig. 3(b) with  $\phi = 1.42\pi$  in Eq. (6), the calculated diffraction pattern agrees well with the data in Fig. 3(a). We plot them separately because they are almost identical. A slight offset of the zero level in the data is attributed to light scattering in the charge-coupled-device (CCD) pixels and a small imbalance in the slit width or the light-amplitude division.

The above analysis gives a rough estimate of the film's thickness. Picking up a single pixel position is the most direct and simple way, but may lead to error in locating the real location of a maximum, due to the presence of the envelope in Eq. (2) and the possible nonuniform responses of the CCD pixels. Therefore, we fit the same experimental data to Eq. (2) with a numerical fitting routine in MATLAB, with the phase  $\phi$  and the constant intensity factor  $I_0$  as the only floating parameters. As a result, we obtain  $\phi = 1.414\pi$ , which gives a thickness value of  $0.710 \mu\text{m}$  through Eq. (1). We see that this  $\phi$  value deviates only by  $3 \text{ nm}$  from the rough estimate above using Eq. (2), which lies within the measurement uncertainty discussed below.

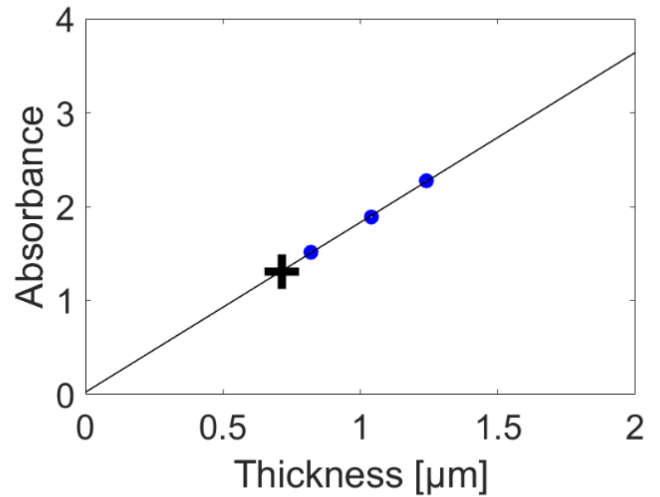


**FIG. 4.** Absorbance of photoresist film at  $\lambda = 279 \text{ nm}$  as a function of thickness. Filled circles: measured points. The absorbance of sample #1 is denoted by a cross (+). The trend line represents optical density as a function of photoresist thickness.

In principle, the uncertainty in the thickness estimation above is determined by the uncertainty of the refractive index of the thin film's material ( $\sim 6 \times 10^{-3}$  here), because  $n_f d$  is determined by Eq. (1) from the measured phase  $\phi$ . The uncertainty in the index in this work comes from the WG-coupling method ( $\sim 10^{-4}$  [6]) and the fluctuation among the samples ( $n_f = 1.63 \pm 0.01$ ). The latter gives the major uncertainty of  $\sim 6 \times 10^{-3}$ , which limits the accuracy of the absolute thickness value of the current sample (photoresist film) by our method, while the former ( $\sim 10^{-4}$ ) can be used to verify the validity of our method using the same sample.

In addition, there are several factors affecting the uncertainty in measuring the phase  $\phi$ , such as the uniformity of film, detection noise due to unwanted internal reflections, nonzero minima, and the finite size of the CCD's pixels. The nonzero minima do not affect our fitting result significantly. We also cannot observe the interference fringes caused by internal reflections, owing to the small index difference between film and substrate (approximately 0.17).

In addition, we move the sample, repeating the experiment and finding no changes in the measured results within the resolution of the CCD pixels, verifying the uniformity of the film.

Finally, the CCD pixel size (interval) could be another major limiting factor in the measurement uncertainty. The phase uncertainty due to finite pixel size can be evaluated from Eq. (6) as follows [7]:

$$\Delta\phi = \sqrt{\left(\frac{\partial\phi}{\partial S}\Delta S\right)^2 + \left(\frac{\partial\phi}{\partial D}\Delta D\right)^2} = \frac{2\pi}{D} \sqrt{(\Delta S)^2 + \left(\frac{S}{D}\Delta D\right)^2}, \quad (7)$$

where  $\Delta S$  and  $\Delta D$  are the uncertainties involved in locating the maxima at specific pixels, both of which may be set to 0.5. Then Eq. (7) is simplified to

$$\Delta\phi = \frac{\pi}{D} \sqrt{1 + \left(\frac{S}{D}\right)^2}. \quad (8)$$

Table 1 shows the error propagation in the estimation of the phase and the thickness of the photoresist film (sample #1), according to Eq. (8). The resultant uncertainties are 2.5% for both phase and thickness. The fractional errors are the same because the uncertainty due to the sample-to-sample index fluctuation was not considered in this table. If we were to include this contribution (estimated to be 12 nm, based on Eq. (1)), the uncertainty in the absolute thickness would be  $\sqrt{18^2 + 12^2} = 22$  nm.

The same experiment is performed on films with different thicknesses, and the thicknesses and refractive index of the thin films are confirmed by the WG-coupling method, using a high-index prism coupler (GGG-prism, Sairontech, SPA-4000) to verify the validity of our experiment and

**TABLE 1.** Uncertainties in the thickness measurement of sample #1

$S$ (pixels)	$D$ (pixels)	$\phi$ (rad)	$d$ (nm)
$23.7 \pm 0.5$	$33.5 \pm 0.5$	$1.414\pi \pm 0.114$	$710 \pm 18$

**TABLE 2.** Comparison of thicknesses of samples #1–5 measured by the WG-coupling method and by double-slit diffraction

Sample	Thickness measured by WG coupling ( $\mu\text{m}$ )	Thickness measured by double-slit diffraction ( $\mu\text{m}$ )	Difference (nm)
#1	0.704	0.710	6
#2	0.820	0.825	5
#3	1.04	1.04	0
#4	1.24	1.24	0
#5	1.74	1.74	0

analysis method. The WG-coupling method can determine thickness and refractive index simultaneously, by measuring the coupling angles of a collimated monochromatic beam into the planar waveguide formed by the thin film [6]. In the WG-coupling experiment, an average index value of  $1.63 \pm 0.01$  is obtained together with film thicknesses. The error in thickness measurement with the WG-coupling method is reported to be  $\sim 20$  nm [6], which is similar to that for the double-slit method (18 nm). As a result, the thicknesses measured by the double-slit diffraction experiments deviates from those measured by the WG-coupling method by 6 nm or less, as shown in Table 2, validating the double-slit method. Note that the deviations are within the uncertainty range discussed above.

Finally, an attempt is made to measure the thickness of a very thin film. A double-slit diffraction pattern for sample #6 is shown in Fig. 5. Because this thin film does not support any waveguide mode, it is impossible to compare the result with that from the WG-coupling method. A phase of  $\phi = 0.121\pi$  is obtained by analyzing the fringes as above. Possible thicknesses satisfying this phase difference are 60 nm, 1.07  $\mu\text{m}$ , 2.07  $\mu\text{m}$ , ... , among which 60 nm is chosen to be the correct one because the measured absorbance indicates that the thickness lies in the range of 0–0.5  $\mu\text{m}$  (see Fig. 4). In Table 3, the error in phase evaluation is calculated to be 0.095 using Eq. (8), which amounts to a fractional error of 25%, resulting in the same fractional error in the thickness evaluation. Such a large fractional error can be expected for a very thin film, considering that the diffraction pattern shifts just a few pixels, as shown in Fig.

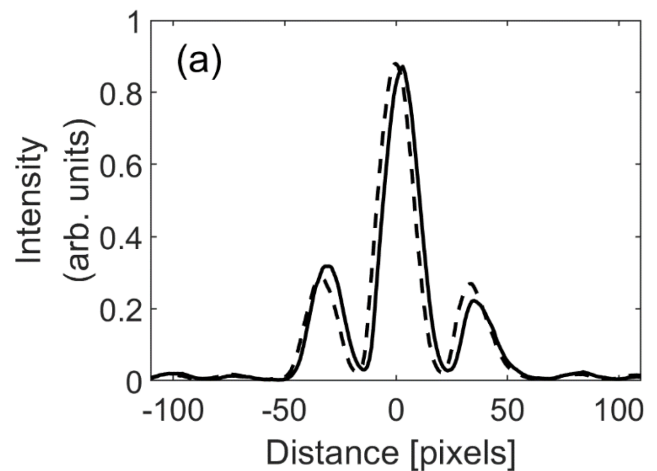


**FIG. 5.** Experimental diffraction patterns of sample #6 (solid line) and the reference sample (dashed line).

**TABLE 3.** Uncertainties in the thickness measurement of sample #6

$S$ (pixels)	$D$ (pixels)	$\phi$ (rad)	$d$ (nm)
$2.0 \pm 0.5$	$33.4 \pm 0.5$	$0.121\pi \pm 0.095$	$60 \pm 15$



5, while the error in the phase evaluation is bounded by a constant value of  $\pi/D$ , as given in Eq. (8).

#### IV. DISCUSSION

Since the phase  $\phi$  is in principle estimated from the measured  $S$  and  $D$  values through Eq. (6), the uncertainty in the phase measurement is determined mainly by the resolution of the CCD array. As shown in Tables 1 and 3, a smaller pixel spacing would give a smaller phase-measurement error. In the current experimental arrangement, the distance  $D$  between the central and the next maximum of the diffraction pattern for the reference sample is around  $33 \pm 0.5$  pixels. The 0.5-pixel error in locating the diffraction maxima corresponds to a phase error of at least 0.095, which is equivalent to a thickness error of 15 nm.

For a fixed CCD pixel spacing ( $8 \mu\text{m}$  for our CCD), it is possible to increase the width of the diffraction pattern to reduce the measurement uncertainty. Factors affecting the width of the pattern are the slit separation, the wavelength of the incident light, and the distance between the CCD plane and the slit (or lens L2). For a fixed wavelength, the diffraction pattern is more widely spread for a smaller slit separation and a larger slit-to-screen distance. Using a lens of longer focal length (1 m in this experiment) would increase the screen-to-slit (or -lens) distance, which in turn would broaden the diffraction pattern, reducing the measurement uncertainty as a result (see Appendix).

Our method has advantages over the other methods for measuring thin-film thickness; some of them are that the double-slit method is noncontact (compared to the mechanical scanning of a probe), vibration-insensitive (compared to Michelson interferometry), and simple and low-cost (compared to electron microscopy). Our method could also measure a very thin film, which is not possible with the WG-coupling method. On the other hand, a disadvantage is that refractive-index information is necessary to estimate the film thickness, because the phase is proportional to the product of the film thickness and the refractive-index difference between the film and the atmosphere. Although it works well for materials with a reproducible refractive index, it would be desirable to be able to measure the thickness independently.

#### V. CONCLUSION

We have applied a double-slit experiment to measure the thickness of a thin film when the refractive index is known. With proper arrangement of optical elements we could obtain Fraunhofer diffraction, which made possible a simple and accurate estimation of film thickness, without requiring a lithographically defined phase step or critical alignment. Because the relative shift of the principal maximum of the diffraction pattern was measured with respect to the fringe spacing of a reference sample, our method was free from the errors involved in measurements of absolute experimen-

tal parameters, such as slit separation and distance to the screen.

As a further study, we can suggest the following methods to measure the film thickness independently from any refractive-index information: using two different surrounding media to cover the phase step, or performing a double-slit experiment in reflection mode.

#### APPENDIX

Here we give a detailed proof of the fact that a Fraunhofer diffraction pattern is formed at the screen plane when  $a$  and  $b$  satisfy the geometrical image-forming relation

$$\frac{1}{a} + \frac{1}{b} = \frac{1}{f}, \quad (\text{A1})$$

by calculating the diffracted electric field amplitudes in the Fresnel approximation at the planes shown in Fig. 1, represented by two-dimensional Cartesian coordinates  $(x_1, y_1)$ ,  $(x_2, y_2)$ , and  $(x_3, y_3)$  respectively [8].

The electric field just before the slits can be expressed as

$$E(x_1, y_1) = P(x_1, y_1) e^{i \frac{\pi}{\lambda d_1} (x_1^2 + y_1^2)}, \quad (\text{A2})$$

where  $P(x_1, y_1)$  is the aperture function of the object (slits and film), and the phase factor represents the wavefront of the Gaussian beam emerging from the beam waist located at a distance  $d_1$  from the object. After propagating a distance  $d_2$ , the electric field just before lens L2 can be expressed as

$$E_a(x_2, y_2) = \frac{1}{\lambda d_2} \iint E(x_1, y_1) e^{i \frac{\pi}{\lambda d_2} [(x_2 - x_1)^2 + (y_2 - y_1)^2]} dx_1 dy_1, \quad (\text{A3})$$

omitting the constant phase factor. After passing through the lens, the electric field must be multiplied by the lens transmission function  $t_1(x_2, y_2)$ , resulting in

$$E_b(x_2, y_2) = E_a(x_2, y_2) t_1(x_2, y_2) = \frac{1}{\lambda d_2} \iint P(x_1, y_1) e^{i \frac{\pi}{\lambda d_1} (x_1^2 + y_1^2)} e^{i \frac{\pi}{\lambda d_2} [(x_2 - x_1)^2 + (y_2 - y_1)^2]} e^{-i \frac{\pi}{\lambda f} (x_2^2 + y_2^2)} dx_1 dy_1. \quad (\text{A4})$$

After propagating a distance  $b$  from the lens, the electric field on the screen can be expressed and rearranged as

$$E(x_3, y_3) = \frac{1}{\lambda b} \iint E_b(x_2, y_2) e^{i \frac{\pi}{\lambda b} [(x_3 - x_2)^2 + (y_3 - y_2)^2]} dx_2 dy_2 = \frac{1}{\lambda^2 b d_2} \iint \iint P(x_1, y_1) e^{i \frac{\pi}{\lambda} \left[ \frac{(x_1^2 + y_1^2)}{d_1} + \frac{(x_2^2 + y_2^2)}{d_2} + \frac{(x_3^2 + y_3^2)}{b} - \frac{(2x_1 x_2 + 2y_1 y_2)}{d_2} \right]} \times e^{i \frac{\pi}{\lambda} \left[ -\frac{(x_2^2 + y_2^2)}{f} + \frac{(x_2^2 + y_2^2)}{b} - \frac{(2x_2 x_3 + 2y_2 y_3)}{b} \right]} dx_1 dy_1 dx_2 dy_2. \quad (\text{A5})$$

Using the image-forming relation in Eq. (A1), this can be simplified to give

$$\begin{aligned}
E(x_3, y_3) &= \frac{1}{\lambda^2 b d_2} \iint_{-\infty}^{\infty} e^{i \frac{\pi d_1}{\lambda a d_2} (x'^2 + y'^2)} dx' dy' \\
&\iint P(x_1, y_1) e^{-i \frac{2\pi a}{\lambda b d_1} (x_3 x_1 + y_3 y_1)} dx_1 dy_1, \quad (\text{A6})
\end{aligned}$$

where  $x' \equiv x_2 - \frac{a d_2}{d_1} \left( \frac{x_1}{d_2} + \frac{x_3}{b} \right)$  and  $y' \equiv y_2 - \frac{a d_2}{d_1} \left( \frac{y_1}{d_2} + \frac{y_3}{b} \right)$ .

The definite integral over  $x'$  can be evaluated to give a Fresnel integral

$$\int_{-\infty}^{\infty} e^{i \frac{\pi d_1}{\lambda a d_2} x'^2} dx' = \sqrt{\frac{\lambda a d_2}{\pi d_1}} \left( 2 \int_0^{\infty} e^{i v^2} dv \right) = \sqrt{\frac{\lambda a d_2}{2 d_1}} (1 + i), \quad (\text{A7})$$

and likewise for the integration over  $y'$ . Therefore, we finally obtain the diffracted electric field amplitude on the screen within the Fresnel approximation:

$$E(x_3, y_3) = i \frac{a}{\lambda b d_1} \iint P(x_1, y_1) e^{-i \frac{2\pi a}{\lambda b d_1} (x_3 x_1 + y_3 y_1)} dx_1 dy_1. \quad (\text{A8})$$

This is the Fourier transformation of the aperture function  $P(x_1, y_1)$  with a set of spatial frequencies

$$f_x = \frac{a x_3}{\lambda b d_1} \text{ and } f_y = \frac{a y_3}{\lambda b d_1}. \quad (\text{A9})$$

When the lens is placed very close to the object,  $d_1 \cong a$  and  $f_x \cong x_3/\lambda b$ . Therefore, the width of the Fraunhofer diffraction pattern is proportional to the lens-to-screen distance  $b$ , and inversely proportional to the separation between the two slits.

## ACKNOWLEDGMENT

This work was supported by the Basic Science Research

Program of the National Research Foundation of Korea (NRF) (2016R1D1A3B01006903), and the MSIT (Ministry of Science and ICT), Korea, under the ITRC (Information Technology Research Center) support program (IITP-2020-0-01606) supervised by the IITP (Institute of Information & Communications Technology Planning & Evaluation).

## REFERENCES

1. T. Young, "The bakerian lecture: experiments and calculations relative to physical optics," *Phil. Trans. R. Soc. London* **94**, 1–16 (1804).
2. J.-A. Kim, J. W. Kim, T. B. Eom, J. Jin, and C.-S. Kang, "Vibration-insensitive measurement of thickness variation of glass panels using double-slit interferometry," *Opt. Express* **22**, 6486–6494 (2014).
3. J. Emile and O. Emile, "Mapping of the Marangoni effect in soap films using Young's double-slit experiment," *Europhys. Lett.* **104**, 14001 (2013).
4. A. Lipson, S. G. Lipson, and H. Lipson, *Optical Physics*, 4<sup>th</sup> ed., (Cambridge University Press, Cambridge, UK. 2011), pp. 279–280.
5. F. L. Pedrotti, L. M. Pedrotti, and L. S. Pedrotti, *Introduction to Optics*, 3<sup>rd</sup> ed., (Addison Wesley, MA, USA. 2006), pp. 268–271.
6. R. Ulrich and R. Torge, "Measurement of thin film parameters with a prism coupler," *Appl. Opt.* **12**, 2901–2908 (1973).
7. Guide to the expression of uncertainty in measurement, ISO/IEC GUIDE 98-3:2008/SUPPL 1:2008, International, International Organization for standardization, Geneva, Switzerland (Nov. 2008).
8. J. W. Goodman, *Introduction to Fourier Optics*, 2<sup>nd</sup> ed., (McGraw-Hill, NY, USA. 1996), pp. 55–107, (Transl.: in N. Kim, Ed., *Introduction to Fourier Optics*, Interscience, Seoul, Korea. 2000, pp. 66–120).